Available online at www.sciencedirect.com
ScienceDirect
Analytical Biochemistry 375 (2008) 345–353
ANALYTICAL BIOCHEMISTRY
www.elsevier.com/locate/yabio

Bienzyme amperometric biosensor using gold nanoparticle-modified electrodes for the determination of inulin in foods

Javier Manso, M[a] Luz Mena, P. Yáñez-Sedeño *, José M. Pingarrón

Department of Analytical Chemistry, Faculty of Chemistry, University Complutense of Madrid, 28040 Madrid, Spain

Received 29 November 2007
Available online 23 December 2007

Abstract

A biosensor design involving coimmobilization of fructose dehydrogenase (FDH) and inulinase (INU) on a gold nanoparticle–cysteamine (Cyst) self-assembled monolayer (SAM)-modified gold electrode (Au_{coll}–Cyst–AuE), for the determination of the carbohydrate inulin in foodstuffs, is reported. Tetrathiafulvalene (TTF), used as the mediator, was also coimmobilized by crosslinking with glutaraldehyde. INU catalyzes the hydrolysis of inulin, forming fructose that is detected through the fructose dehydrogenase system by the electrochemical oxidation of TTF at the bioelectrode. The variables involved in the preparation and performance of both the single enzyme FDH biosensor and the bienzyme inulin biosensor were optimized. The FDH–Au_{coll}–Cyst–AuE biosensor exhibited rapid and sensitive response to fructose, allowing the obtention of improved analytical characteristics for the determination of fructose with respect to other FDH electrochemical biosensors. Moreover, the lifetime of this biosensor was 35 days. The bienzyme INU/FDH–Au_{coll}–Cyst–AuE biosensor provided a calibration plot for inulin in the (5–100) $\times 10^{-6}$ M linear range, with a detection limit of 6.6×10^{-7} mol L^{-1}. One single bienzyme biosensor responded within the control limits, set at $\pm 3\times$ the standard deviation of the currents measured on the first day of use, for more than 5 months. Furthermore, the biosensor exhibited high selectivity with respect to other carbohydrates. The usefulness of the biosensor was evaluated by the rapid determination of inulin in food products involving minimization of the fructose interference.

Keywords: Gold nanoparticles; Self-assembled monolayer; Inulin; Bienzyme amperometric biosensor

The suitable immobilization of biomolecules is a crucial step in the preparation of biosensors and, in particular, of electrochemical biosensors. The immobilization approaches require preserving the stability and biological activity of the biomolecules as well as their orientation, distribution, and proximity to the electrode surface and reaction substrate. Due to the unique properties of gold nanoparticles, nanostructured electrodes with this nanomaterial have been demonstrated to be a versatile and powerful tool to construct biosensors that accomplish such requirements [1,2]. In particular, advantages in biocompatibility, stability, sensitivity, possibility of electrocatalysis, and easiness of sensor preparation have been claimed as being derived from the use of gold nanoparticles. Furthermore, electrode modification with self-assembled monolayers (SAMs)[1] constitutes a simple method for the fabrication of functionalized surfaces with controlled com-

* Corresponding author. Fax: +34 91 3944329.
E-mail address: yseo@quim.ucm.es (P. Yáñez-Sedeño).

[1] *Abbreviations used*: SAM, self-assembled monolayer; Cyst, cysteamine; FDH, fructose dehydrogenase; INU, inulinase; GFR, glomerular filtration rate; TLC, thin-layer chromatography; TTF, tetrathiafulvalene; GPES, general-purpose electrochemical system; AuE, gold electrode; Au_{coll}, colloidal gold; PQQ, pyrrolequinolin quinone; LOD, limit of detection; RSD, relative standard deviation; CA, cellulose acetate; GCE, glassy carbon electrode; MPA, mercaptopropionic acid; CPE, carbon paste electrode.

0003-2697/$ - see front matter © 2007 Elsevier Inc. All rights reserved.
doi:10.1016/j.ab.2007.12.020

position, structure, and thickness. These SAMs can be further used to attach gold nanoparticles and/or enzymes to the electrode surface [3,4].

In a previous work [5], we reported on the preparation of glucose oxidase biosensors based on gold nanoparticles bound to different SAMs and found that a design involving colloidal gold and a cysteamine (Cyst) SAM on a gold electrode substrate exhibited good sensitivity for the determination of glucose as well as high stability of the biosensor. In this article, a similar biosensor construction strategy was employed to develop a bienzyme electrode involving fructose dehydrogenase (FDH) and inulinase (INU) for the determination of inulin in food products.

Inulin (Fig. 1) is a fructan carbohydrate in which most of the glycosidic bonds are fructosyl–fructose, and that usually possesses a terminal glucose unit [6]. It occurs as a reserve carbohydrate in chicory and asparagus roots, Jerusalem artichoke, and garlic. This polysaccharide belongs to the group of fructo-oligosaccharides and is a source for the production of fructose [7]. It is also used to obtain oligofructose, a prebiotic with positive effects on human health [8], and it is added as a bioactive ingredient to functional foods to promote the appearance of bifidus and other beneficial microorganisms, thereby creating a healthy effect in the human body through the intestinal flora.

The determination of inulin is of great interest in the food industry, not only for the monitoring of the extraction process of this polysaccharide from its raw material but also for the monitoring of fructose production from the polysaccharide. Moreover, methods for the determination of inulin as an ingredient of diethetic and children's foods in which this compound constitutes a part of the dietary fiber are required.

Table 1 summarizes the analytical characteristics of the methods developed for the determination of inulin [9–23]. Because of the use of inulin in clinical practice for determination of the glomerular filtration rate (GFR), various liquid chromatographic methods using UV [17,19,20], refractive index [15,16], light scattering [12], and electrochemical detection [10,22] have been developed, with most of them being applied to the analysis of inulin in plasma and urine. Thin-layer chromatography (TLC) has also been used for the determination of fructo-oligosaccharides in biological tissues [8] and of inulin in food samples [13]. Most of the methods for the determination of inulin are based on reactions with the fructose derived from hydrolysis. Enzymatic methods based on the hydrolysis of inulin by INU to give fructose were developed accordingly [9,11,14,23]. In various approaches, after fructose is formed, it is phosphorylated by adenosine-5β-triphosphate and hexokinase and isomerized to glucose-6-phosphate by phosphoglucose isomerase. Glucose-6-phosphate is oxidized to gluconate-6-phosphate by glucose-6-phosphate dehydrogenase, and the NADH formed in this sequence of reactions is determined spectrophotometrically. Warm water has been employed to extract inulin from foodstuffs such as yogurt, honey, cereals, meat, and cake [13–16]. The sample solution was hydrolized in acid media, and fructose was determined in the hydrolysate. The amount of inulin was calculated as the difference between the amount of fructose in the sample before and after hydrolysis.

To the best of our knowledge, the bienzyme biosensor developed in this work is the first sensor configuration described in the literature for determining inulin. The preparation and performance of the electrochemical biosensor constructed by immobilizing FDH and INU onto a gold

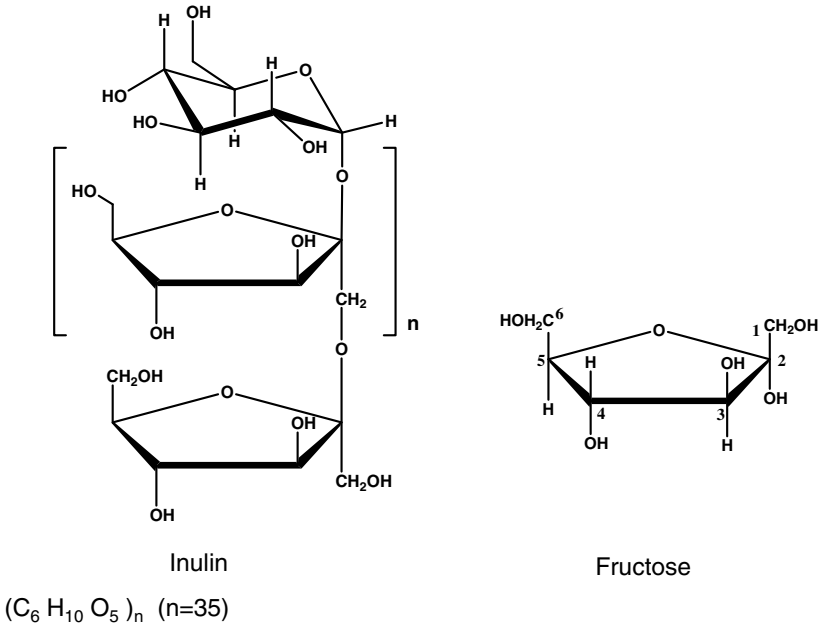

Fig. 1. Chemical structure of inulin.

Table 1
Analytical characteristics of methods developed for the determination of inulin

Technique	Sample	Interferences	Linear range (g L^{-1})	LOD (g L^{-1})	RSD (%)	Reference
Spectrophotometric	Plasma, urine	—	Up to 2	—	< 3	[9]
HPLC–ED	Plasma, urine	Proteins, glucose	0.005–0.3	0.005	—	[10]
Enzymatic–UV	Chicory, diet foods	Glucose, fructose, sucrose, maltose	< 0.7	—	3	[11]
HPLC–ELCD	Plasma, urine	—	—	0.005	< 5	[12]
TLC–Vis	Yogurt, cookies, chocolate	Fructose	—	—	—	[13]
Enzymatic–UV	Cereals, paste	Sucrose	—	1%	5.9	[14]
HPLC–RI	Diet foods, milk	—	< 10	0.05	< 5	[15]
HPLC–RI	Meat products	Fructose	2.8–60 μg	0.82 μg	5.2	[16]
HPLC–UV	Plasma, urine	—	0.2–3.2	0.1	3.3	[17]
TLC–RD	Biological tissues	—	—	—	3	[18]
HPLC–UV	Plasma, urine	—	0.1–3.2	0.001	10	[19]
HPLC–UV	Plasma, urine	—	0.012–0.1	0.012	11	[20]
Spectrophotometric	Plasma	Sucrose	0.5–4	—	15	[21]
HPLC–ED	Plasma, urine	—	0.005–0.2	0.001	5	[22]
Enzymatic–UV	Plasma	Glucose	—	—	1	[23]

Note. ED, electrochemical detection; ELCD, electrolytic conductivity detection; RI, refractive index.

nanoparticle–Cyst SAM-modified gold electrode are discussed, and the analytical characteristics of the methods for the determination of fructose and inulin are established. Furthermore, the bienzyme biosensor was applied to the rapid determination of inulin in foodstuffs.

Materials and methods

Aqueous 0.01 mol L^{-1} inulin stock solutions were prepared from the product (inulin from chicory, Sigma, 99%) dissolved in warm water. The enzymes used were INU from *Aspergillus niger* (Fluka, EC 3.2.1.7, 26.7 U/mg) and FDH from *Gluconobacter* sp. (Sigma, EC 1.1.99.11, 41.2 U/mg). D-(−)-Fructose, glucose, D-(+)-maltose monohydrate, D-(+)-galactose, β-lactose, and D-(+)-sucrose all were obtained from Sigma or Fluka (99%). Glucose (Panreac, 99%) and D-(+)-dextrose (Kerfoots) also were used. Colloidal gold was prepared as reported previously [5]. Briefly, 2.5 ml of 1% sodium citrate solution was added to 100 ml of a boiling aqueous solution containing 1 ml of 1% (w/w) $HAuCl_4$ (Sigma, > 49% as Au). The diameter of gold nanoparticles, measured by electron scanning microscopy, was 16 ± 2 nm. Tetrathiafulvalene (TTF), cysteamine hydrochloride, and glutaraldehyde all were obtained from Sigma. Phosphate buffer solution from Scharlau (99%) also was used. Samples analyzed were water-soluble chicory powder "Leroux" (18.5% inulin) and a prebiotic food "Mas Vital" (Pascual, 2.0% inulin). Bio-Gel P-6 Bio-Rad cartridges were used for the treatment of food samples. These cartridges were conditioned by passing 0.05 mol L^{-1} phosphate solution (pH 4.5) at a flow rate of 0.5 ml min^{-1} for 30 min.

Electrochemical measurements were performed using a PGSTAT 12 potentiostat from Autolab with the general-purpose electrochemical system (GPES) electrochemical software (EcoChemie). A three-electrode cell (BAS VC-2 10-ml glass electrochemical cell) equipped with a platinum wire counter electrode (BAS MW-1032), a BAS MF-2063 Ag/AgCl/3M KCl reference electrode, and the biosensor as the working electrode was used. All experiments were performed at room temperature.

Preparation of bienzyme INU/FDH–Au_{coll}–Cyst–AuE biosensor

The gold electrode (AuE) was first pretreated as described previously [24]. Then the clean AuE was immersed in a 0.1 mol L^{-1} Cyst aqueous solution for 2 h in darkness at room temperature [5]. Then the modified electrode, Cyst–AuE, was thoroughly rinsed with water to remove physically adsorbed Cyst. After the electrode was dried, it was immersed in a colloidal gold dispersion, prepared as described above, for 30 min at 4 °C.

The enzymes FDH and INU, as well as the mediator TTF, were coimmobilized by adsorption and crosslinking with glutaraldehyde. First, the colloidal gold (Au_{coll})–Cyst–AuE was coated with 3 μl of 10 U μl^{-1} FDH solution. After the electrode surface had dried, 5 μl of 5.34 U μl^{-1} INU solution was deposited on it. Finally, 3 μl of 0.5 mol L^{-1} TTF solution was incorporated onto the dry surface and the TTF–INU/FDH–Au_{coll}–Cyst–AuE was immersed in a 25% glutaraldehyde solution for 1 h at room temperature. The biosensor was then washed with Milli-Q water and kept in 0.05 mol L^{-1} phosphate solution (pH 4.5) at 4 °C until use.

Determination of inulin in food samples

Water-soluble chicory powder

First, 0.27 g of the sample containing 18.5% inulin was weighed and dissolved in 10 ml of 0.05 mol L^{-1} phosphate solution (pH 4.5) by heating up to 60 °C. Then 2 ml of the

resulting solution was passed through a Bio-Gel P-6 Bio-Rad cartridge and eluted with 0.05 mol L^{-1} phosphate solution at a flow rate of 0.5 ml min^{-1}. The fraction eluted between 6 and 7 min was collected and analyzed by applying the standard additions method. So, 100 μl of the eluate was transferred to the electrochemical cell containing 10 ml of phosphate buffer (pH 4.5). Successive additions of 1.0×10^{-5} mol L^{-1} inulin were carried out as standard additions.

Prebiotic food Mas Vital

The procedure described above was applied to 2.5 g of the sample that was weighed and diluted in 10 ml of 0.05 mol L^{-1} phosphate solution (pH 4.5).

Results

The bienzyme biosensor that was constructed for the determination of inulin implied the immobilization of both INU and FDH onto an Au_{coll}–Cyst–AuE electrode. Fig. 2A shows the steps involved in the preparation of the bienzyme biosensor. As can be observed, once the Cyst SAM was formed on the AuE surface, gold nanoparticles were adsorbed. Then FDH and INU enzymes, as well as TTF, were successively incorporated onto the modified electrode. Finally, both enzymes and the mediator were coimmobilized by using glutaraldehyde as a crosslinker agent, thereby forming a three-dimensional assembly in which the mediator is entrapped [24] (not shown). Fig. 2B illustrates the biosensor functioning. The enzyme INU catalyzes inulin endohydrolysis reaction to form fructose. Then fructose oxidation is specifically catalyzed by FDH, giving rise to the reduction of the enzyme PQQ (pyrrolequinolin quinone) group to H_2PQQ. H_2PQQ is reoxidized by means of the oxidized form of the mediator, TTF^+, and the electrochemical oxidation of TTF at the bioelectrode is used for monitoring of the overall reaction.

The development of the TTF–INU/FDH–Au_{coll}–Cyst–AuE biosensor required as a first step the preparation and evaluation of a single enzyme FDH bioelectrode, TTF–FDH–Au_{coll}–Cyst–AuE. This was carried out by optimization of the variables implied in the construction of the biosensor by checking the detection of fructose amperometrically.

Construction and performance of TTF–FDH–Au_{coll}–Cyst–AuE biosensor

A fabrication procedure similar to that described earlier (except for the INU incorporation) was followed to prepare the FDH biosensor. The immersion time of the Cyst–AuE in the colloidal gold dispersion was optimised first. Various TTF–FDH–Au_{coll}–Cyst–AuE biosensors were constructed by varying the immersion times between 30 min and 4 h, and the slopes of the calibration graphs obtained for fructose in the 1.0×10^{-5} to 1.0×10^{-4} mol L^{-1} concentration range were compared. The results obtained (not shown) demonstrated that no significant differences in the slope values were found over the studied range; therefore, 30 min was selected as the working time for the adsorption of gold nanoparticles.

The influence of the applied potential to the biosensor for the amperometric detection of fructose was evaluated. Fig. 3 shows that the catalytic current increased from 0 V up to a maximum value of +0.2 V. The further decrease of the amperometric response at more positive potential values can be attributed to the nonreversible oxidation of TTF^+ to TTF^{2+} that decomposes and leaks on electrode surface.

The FDH enzyme loading was also optimized by testing the slope values obtained for fructose in the 1.0×10^{-5} to 1.0×10^{-4} mol L^{-1} concentration range with different biosensors constructed by immobilizing 0, 10.8, 18, 30, and 50

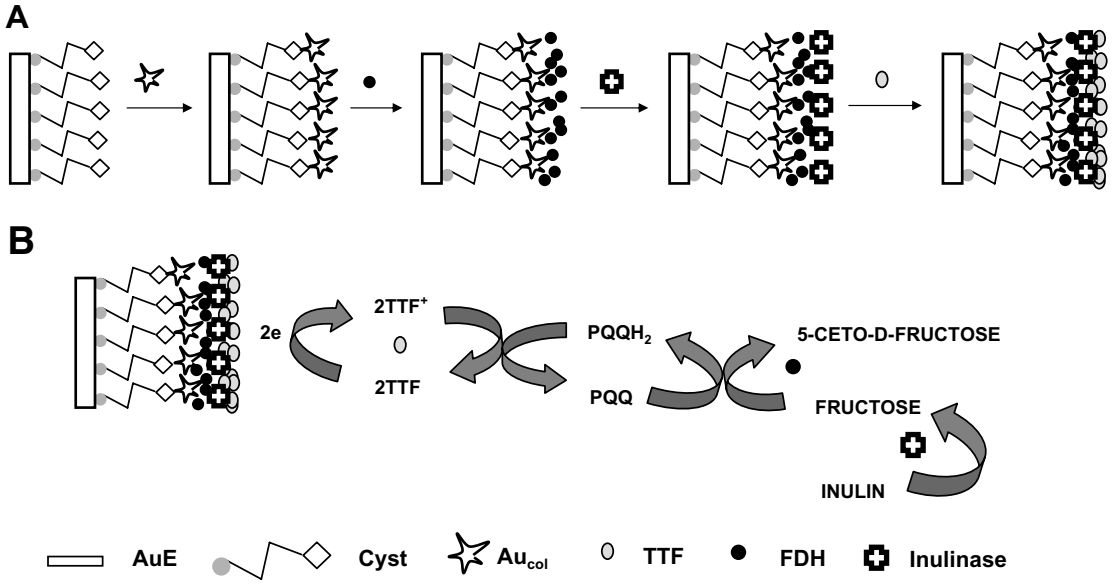

Fig. 2. (A) Steps involved in the preparation of the TTF–INU/FDH–Au_{coll}–Cyst–AuE biosensor. (B) Scheme of the biosensor functioning.

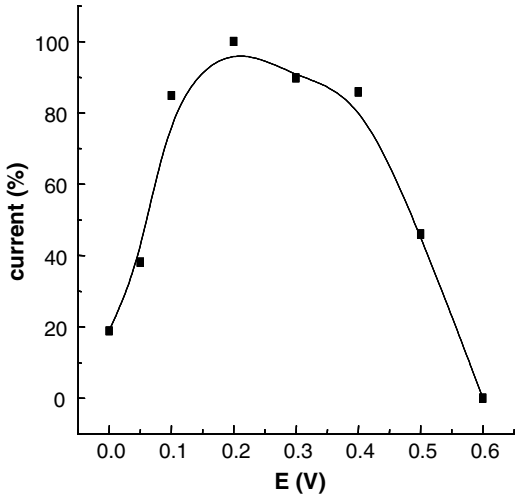

Fig. 3. Effect of the applied potential to the TTF–FDH–Au_{coll}–Cyst–AuE biosensor on the steady-state current for 5.0×10^{-5} mol L^{-1} fructose in 0.05 mol L^{-1} phosphate solution (pH 4.5).

U FDH. The results obtained (not shown) indicated that the best sensitivity was achieved when using 50 U FDH. However, a 30-U enzyme loading was selected for further work because the slope of the fructose calibration graph for fructose was only slightly lower in this case.

The influence of pH on the amperometric response of the biosensor showed that the highest currents were obtained in the pH 4.5 to 5.5 range, in agreement with the best enzyme activity of FDH [25].

Under the working conditions selected above, a linear calibration plot for fructose ($r = 0.996$) was obtained with the TTF–FDH–Au_{coll}–Cyst–AuE biosensor. The corresponding analytical characteristics are summarized in Table 2. The limit of detection (LOD), 0.53 μM, was calculated according to the $3s_b/m$ criterion, where s_b is estimated as the standard deviation ($n = 10$) of the amperometric signals corresponding to different solutions of fructose at the lowest concentration level in the range of linearity (i.e., 5 μM) and m is the slope of the calibration graph. A relative standard deviation value (RSD) of 4.9% for 50 μM fructose ($n = 10$) was obtained. A comparison of the analytical characteristics achieved with the TTF–FDH–Au_{coll}–Cyst–AuE biosensor with respect to those reported in the literature for other FDH biosensor designs is made in Table 2. As can be seen, the sensitivity achieved is remarkably higher than that obtained with the other configurations. For example, it is more than one order of magnitude higher than that reported with an FDH–cellulose acetate (CA)–glassy carbon electrode (GCE) biosensor using ferrocene as the mediator [28]. Moreover, the LOD is approximately 45-fold lower than that obtained with a configuration based on the immobilization of FDH onto a 3-mercaptopropionic acid (MPA) SAM-modified AuE [24]. This enhanced sensitivity can be attributed to the presence of gold nanoparticles in the biosensor configuration that gives rise to improved kinetics of the reactions involved in the overall process [29].

The lifetime of one single TTF–FDH–Au_{coll}–Cyst–AuE was checked by performing three daily measurements of 5.0×10^{-4} mol L^{-1} fructose. When not in use, the biosensor was stored at 4 °C in phosphate buffer solution (pH 4.5). Fig. 4A shows a control chart in which the central value was considered as the mean value of the currents measured on the first day. The upper and lower limits of control were set at ± 3× the standard deviation of this target value. For comparison purposes, the results obtained with an FDH biosensor constructed in the absence of gold nanoparticles are displayed in Fig. 4B. As can be observed, current values within the control limits were obtained with the TTF–FDH–Au_{coll}–Cyst–AuE for 35 days, whereas the TTF–FDH–Cyst–AuE biosensor showed a continuous decrease of the electrode response with increasing times, with the current being 20% lower after 15 days. A clear enhanced stability of the biosensor is achieved by using gold nanoparticles as a consequence of the favorable microenvironment for enzyme immobilization retaining its biological activity. This has been attributed to the similarity of such a microenvironment to that of proteins in native systems [30], allowing more freedom in orientation for the immobilized biomolecules [31].

The comparison of the biosensor lifetime with other FDH designs included in Table 2 also reflects the improved behavior of the TTF–FDH–Au_{coll}–Cyst–AuE. For example, only 70% of the initial current was obtained with an FDH–Cyst–AuE configuration using $Co(phen)_2^{2+}$ as the mediator after the first day of biosensor preparation [32]. Moreover, the enzyme reaction at the TTF–FDH–Au_{coll}–Cyst–AuE obeyed Michaelis–Menten kinetics, as deduced from the slope value, $x = 1.03 \pm 0.05$, of the corresponding linear log $[(I_{max}/I) - 1]$ versus log [fructose] plot. The calcu-

Table 2
Electrochemical biosensors for the determination of fructose

Electrode	Mediator	E_{det} (V)	Linear range (mM)	Slope (mA M^{-1})	LOD (μM)	Useful lifetime (days)	K_M^{app}(mM)	Reference
FDH–MPA–AuE	TTF	+0.2	0.01–1.0	1.7	24	30	5.5 ± 0.4	[24]
FDH–CPE	TCNQ	+0.21	0.02–0.8	—	10	1	—	[25]
FDH–CPE	$Os(bPy)_2Cl_2$	+0.1	0.2–20	—	35	7	61	[26]
FDH–ODTNB–AuE	Hydroxymethylferrocene	+0.3	Up to 0.7	—	3	25	—	[27]
FDH–CA–GCE	Ferrocene	+0.3	0.01–0.8	0.23	3	< 9 h	—	[28]
FDH–Cyst–AuE	$Co(phen)_2^{2+}$	+0.3	0.01–0.11	0.15	—	70% second day	—	[30]
FDH–Au_{coll}–Cyst–AuE	TTF	+0.2	0.005–0.1	3.1 ± 0.2	0.53	35	0.59 ± 0.07	This work

Note. ODTNB, 5-(octyldithio)-2-nitrobenzoic acid.

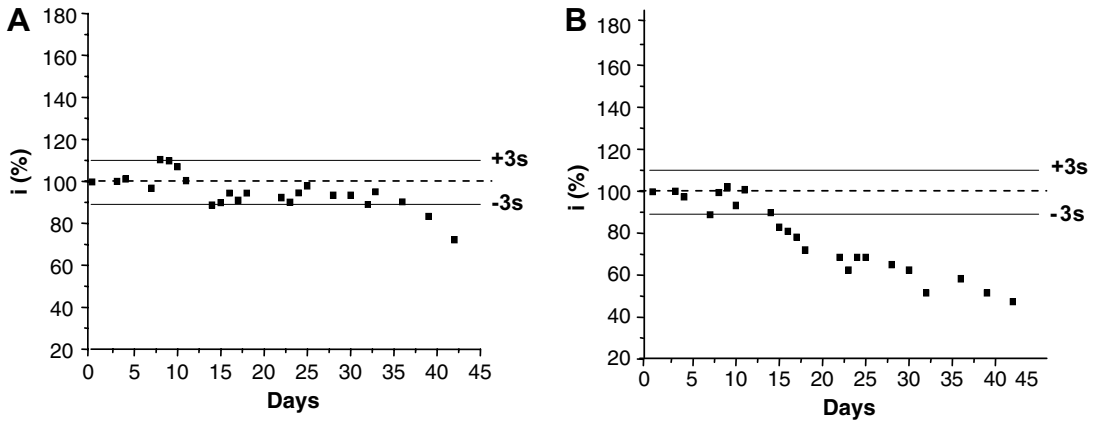

Fig. 4. Control chart constructed for TTF–FDH–Au_{coll}–Cyst–AuE (A) and TTF–FDH–Cyst–AuE (B) biosensors. Data show the mean values of three measurements from different 5.0×10^{-5} mol L^{-1} fructose solutions. $E_{app} = +0.2$ V. Other conditions are as in Fig. 3.

lated value of the apparent Michaelis–Menten constant (K_M^{app}) was 0.59 ± 0.07 mmol L^{-1}, indicating a high enzyme–substrate affinity under the microenvironment provided by gold nanoparticles. As can be deduced from Table 2, this value is 10-fold lower than that obtained with a TTF–FDH–MPA–AuE biosensor [24] and 100-fold lower than that obtained with an FDH–$Os(bPy)^{2+}$/carbon paste electrode (CPE) biosensor [26].

Construction and performance of TTF–INU/FDH–Au_{coll}–Cyst–AuE biosensor

Taking as a basis the FDH biosensor configuration optimized above, the bienzyme INU/FDH biosensor was constructed. Accordingly, the INU loading was optimized. This was accomplished by measuring the slope value obtained for inulin in the 1.0×10^{-5} to 1.0×10^{-4} mol L^{-1} concentration range using different bienzyme biosensors constructed with 30 U FDH and various INU loadings ranging between 0 and 30.5 U. The last value was the highest available INU loading because of the low solubility of the enzyme in the working medium. As Fig. 5 shows, the sensitivity increased with increasing amounts of INU up to approximately 26 U. When the results obtained with 26.7 and 30.5 U were compared, the repeatability of the slope value was remarkably better with the lower loading and; therefore, this INU amount was selected for further work.

The calibration plot for inulin was linear in the (5–100) $\times 10^{-6}$ M concentration range, with a slope value of 2.4 ± 0.1 mA M^{-1} and an LOD of 6.6×10^{-7} M, which is equivalent to 3.3 mg L^{-1} inulin. This value is similar to those values achieved with the most sensitive methods reported in the literature for the determination of inulin (see Table 1) that used HPLC with electrochemical or UV detection [10,22,19]. A limit of determination of 2.2×10^{-6} M (11 mg L^{-1}) was obtained according to the $10 \times s$ criterion. Furthermore, an RSD value of 5.0% was calculated from the slope values of the inulin calibration

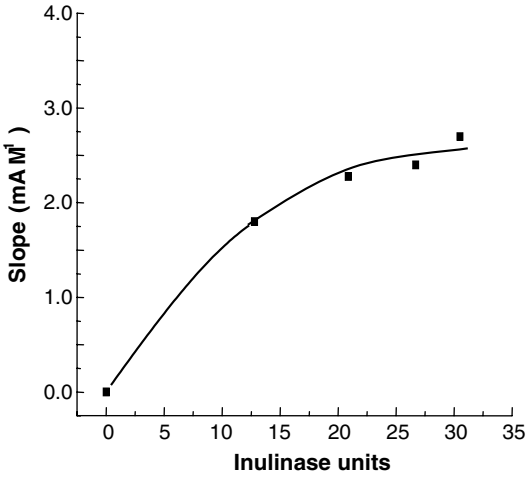

Fig. 5. Effect of INU loading on the slope value of the calibration graph for inulin in the $(0.1 - 1.0) \times 10^{-4}$ mol L^{-1} concentration range obtained with a TTF–INU/FDH–Au_{coll}–Cyst–AuE biosensor. $E_{app} = +0.2$ V. Other conditions are as in Fig. 3.

plots obtained with three different biosensors, indicating good reproducibility in the bienzyme biosensor construction. Moreover, excellent repeatability was achieved, with RSD = 3.6% ($n = 10$) for 5.0×10^{-5} M inulin current measurements.

The bienzyme biosensor for inulin is also characterized by high stability. The control chart depicted in Fig. 6 shows that one single bienzyme biosensor responded within the control limits, set at $\pm$ 3$\times$ the standard deviation of the currents obtained ($n = 3$) on the first day of use, for more than 5 months. When the biosensor was not in use, it was stored in a phosphate buffer solution (pH 4.5) at 4 °C. Moreover, the calculated value of the apparent Michaelis–Menten constant, 1.1 ± 0.2 mM, is much lower than that given for INU immobilized onto Amberlite supports for their use in a reactor for enzyme hydrolysis ($K_M^{app} = 21.6$ mM) [6], and it is very similar to that reported for free INU, $K_M^{app} = 2.57$ mM [33], suggesting that the enzyme immobilization approach did not negatively affect

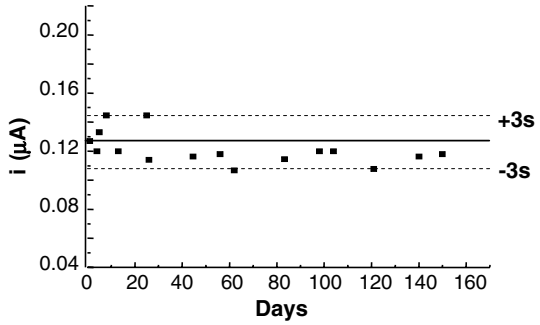

Fig. 6. Control chart constructed for a TTF–INU/FDH–Au_{coll}–Cyst–AuE biosensor. Data show the mean values of three measurements from different 5.0×10^{-5} mol L^{-1} inulin solutions. $E_{app} = +0.2$ V. Other conditions are as in Fig. 3.

the substrate affinity. These results again demonstrate the advantages provided by the presence of gold nanoparticles related to the enzyme reactions occurring under this type of configuration. Finally, the biosensor response time was evaluated as the time elapsed to reach 90% of the steady-state current. As expected, the value obtained, 100 s, is somewhat longer than those values usually observed with single enzyme amperometric biosensors, but it is similar to those values achieved with other bienzyme biosensors [34].

The INU/FDH bienzyme biosensor exhibited high selectivity with respect to other carbohydrates. As Fig. 7 shows, dextrose, glucose, lactose, and maltose gave a significant amperometric response under the conditions employed. Nevertheless, saccharose produced an error of approximately 10% in the determination of inulin that is attributed to weak catalytic activity of the enzyme INU toward the hydrolysis of the O-glycosidic bond of saccharose, with this giving rise to the formation of glucose and fructose. However, this error is not important from a practical point of view because most real samples containing inulin are diethetic products with low-calorie contents and do not contain saccharose. A similar comment can be made about ascorbic acid. Although this compound produced an error of approximately 10% in the inulin amperometric response as a consequence of its electrochemical oxidation at the applied potential, the content of ascorbic acid, if any, in most prebiotic foods is much lower than that of inulin or fructose.

Determination of inulin in food samples

The procedures described in Materials and Methods were used for the determination of inulin in two commercial food products: a water-soluble chicory powder sample Leroux and a prebiotic food Mas Vital. Both samples contained other carbohydrates, including fructose, in relatively high percentages together with inulin. Therefore, a separation step was needed. This was carried out by solid phase extraction using Bio-Gel P-6 Bio-Rad size exclusion cartridges taking advantage of the large difference of molecular weights between fructose (MW 180) and inulin (MW 5000). The elution curves of both compounds were constructed by passing 2.0 ml of 5.0×10^{-2} mol L^{-1} fructose and 1.0×10^{-3} mol L^{-1} inulin stock solutions through the cartridge and eluting with a 0.05 mol L^{-1} phosphate solution (pH 4.5) at a flow rate of 0.5 ml min^{-1}. The fractions eluted were collected every minute and analyzed with the fructose or inulin biosensor by measuring the current from the solutions obtained by taking 100 μl of the eluate and transferring it to the electrochemical cell containing 10 ml of phosphate buffer (pH 4.5). Fig. 8 shows that the highest signal corresponding to inulin was obtained for the frac-

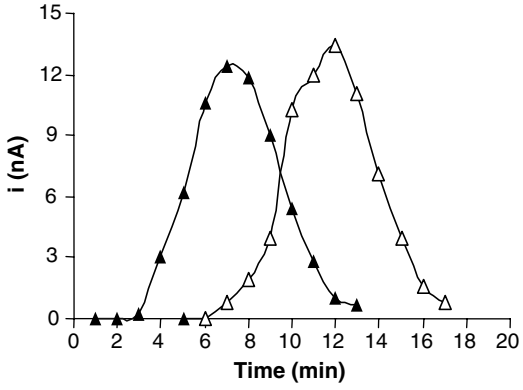

Fig. 8. Elution curves of inulin (▲) and fructose (Δ) from Bio-Gel P-6 Bio-Rad cartridges.

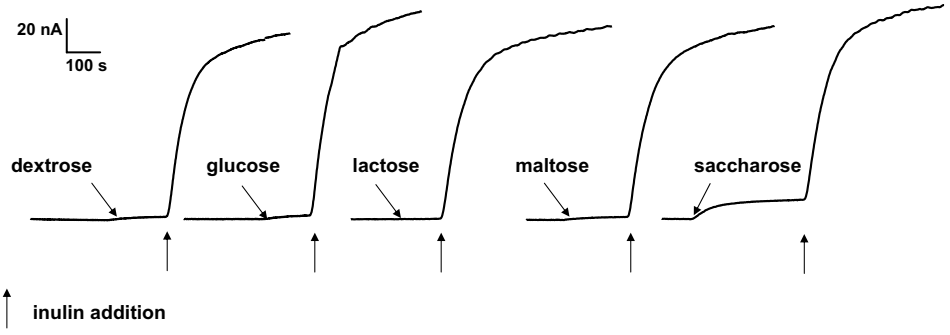

Fig. 7. Current time recordings with a TTF–INU/FDH–Au_{coll}–Cyst–AuE biosensor for 5.0×10^{-5} mol L^{-1} dextrose, glucose, lactose, maltose, and saccharose followed by additions of 5.0×10^{-5} mol L^{-1} inulin. Other conditions are as is Fig. 3.

tion that eluted between 6 and 7 min. Moreover, the current measured with the fructose biosensor for this fraction was much lower than that recorded for inulin. Therefore, this particular fraction was selected to be analyzed in the case of real samples so as to minimize the fructose interference. By applying the standard additions method, following the procedure described in Materials and Methods, the inulin contents obtained were as follows: chicory powder Leroux, $19.5 \pm 0.4\%$, RSD = 2%, $n = 6$; prebiotic food Mas Vital, $1.8 \pm 0.1\%$, RSD = 5%, $n = 6$. These results agree fairly well with the inulin content labeled for each product.

Conclusions

A bienzyme amperometric biosensor for the rapid and selective determination of inulin has been constructed for the first time. The biosensor was designed by using gold nanoparticles as an appropriate microenvironment to efficiently immobilize the biomolecules and to improve the kinetics of the reactions involved in the detection process. The advantages provided by this design led to high sensitivity and stability of the biosensor. The methodology making use of the bienzyme biosensor for the analysis of real samples compares favorably with other analytical methodologies that are more complex and time-consuming, making it an attractive tool to be used in the food industry.

Acknowledgment

Financial support from the Ministerio de Educación y Ciencia (projects CTQ2006-02905 and CTQ2006-02743) is gratefully acknowledged.

References

[1] J. Wang, Nanomaterial-based electrochemical biosensors, Analyst 130 (2005) 421–426.
[2] M. Pumera, S. Sánchez, I. Ichinose, J. Tang, Electrochemical nanobiosensors, Sens. Actuat. B 123 (2007) 1195–1205.
[3] A.N. Shipway, M. Lahav, I. Willner, Nanostructured gold colloid electrodes, Adv. Mater. 12 (2000) 993–998.
[4] Y. Xiao, H.X. Ju, H.Y. Chen, Hydrogen peroxide sensor based on horseradish peroxidase-labeled Au colloids immobilized on gold electrode surface by cysteamine monolayer, Anal. Chim. Acta 391 (1999) 73–82.
[5] M.L. Mena, P. Yáñez-Sedeño, J.M. Pingarrón, A comparison of different strategies for the construction of amperometric enzyme biosensors using gold nanoparticle-modified electrodes, Anal. Biochem. 336 (2005) 20–27.
[6] J.R. Rocha, R. Catana, B.S. Ferreira, J.M.S. Cabral, P. Fernandes, Design and characterisation of an enzyme system for inulin hydrolysis, Food Chem. 95 (2006) 77–82.
[7] H. Millo, M.J. Werman, Hepatic fructose-metabolizing enzymes and related metabolites: Role of dietary copper and gender, J. Nutr. Biochem. 11 (2000) 374–381.
[8] N. Kaur, A.K. Gupta, Applications of inulin and oligofructose in health and nutrition, J. Biosci. 27 (2002) 703–714.
[9] O. Sugita, Y. Tomiyama, T. Matsuto, M. Okada, F. Gejyo, M. Arakawa, S. Takahashi, Y. Watazu, N. Kaneda, A new enzymatic method for the determination of inulin, Ann. Clin. Biochem. 32 (1995) 561–565.
[10] R. Sechaud, L.A. Decosterd, A. Pechere Bertschi, J. Biollaz, U.W. Kesselring, Determination of the polyfructosan sinistrin in biological fluids by HPLC with electrochemical detection, J. Pharm. Biomed. Anal. 14 (1996) 483–490.
[11] K. Hofer, D. Jenewein, Enzymatic determination of inulin in food and dietary supplements, Eur. Food Res. Technol. 209 (1999) 423–427.
[12] R. Marsilio, M. Naturale, P. Manghi, G. Montini, L. Murer, M. Ros, G. Bisogno, B. Andretta, N. Dussini, G. Giordano, G. Zacchello, R. Dall'Amico, Rapid and simple determination of inulin in biological fluids by high-performance liquid chromatography with light-scattering detection, J. Chromatogr. B 744 (2000) 241–247.
[13] B. Simonosvka, Determination of inulin in foods, J. AOAC Intl. 83 (2000) 675–678.
[14] M. Steegmans, S. Iliaens, H. Hoebregs, Enzymatic, spectrophotometric determination of glucose, fructose, sucrose, and inulin/oligofructose in foods, J. AOAC Intl. 87 (2004) 1200–1207.
[15] A. Zuleta, M.E. Sambucetti, Inulin determination for food labeling, J. Agric. Food Chem. 49 (2001) 4570–4572.
[16] S. Vendrell-Pascuas, A.I. Castellote-Bargallo, M.C. Lopez-Sabater, Determination of inulin in meat products by high-performance liquid chromatography with refractive index detection, J. Chromatogr. A 881 (2000) 591–597.
[17] R. Dall'Amico, G. Montini, L. Pisanello, G. Piovesan, S. Bottaro, A.T. Cracco, G. Zacchello, F. Zacchello, Determination of inulin in plasma and urine by reversed-phase high-performance liquid chromatography, J. Chromatogr. B 672 (1995) 155–159.
[18] K. Reiffová, R. Nemcová, Thin-layer chromatography analysis of fructooligosaccharides in biological samples, J. Chromatogr. A 1110 (2006) 214–221.
[19] A. Pastore, S. Bernardini, L. Dello Strologo, G. Rizzoni, C. Cortese, G. Federici, Simultaneous determination of inulin and *p*-aminohippuric acid in plasma and urine by reversed-phase high-performance liquid chromatography, J. Chromatogr. B 751 (2001) 187–191.
[20] N. Baccard, G. Hoizey, G. Hoizey, C. Frances, D. Lamiable, T. Trenque, H. Millart, Simultaneous determination of inulin and *p*-aminohippuric acid (PAH) in human plasma and urine by high-performance liquid chromatography, Analyst 124 (1999) 833–836.
[21] T.D. Nolin, I.V. Colaizzi, P.M. Palevsky, G.R. Matzke, R.F. Frye, Rapid microtiter plate assay for determination of inulin in human plasma and dialysate, J. Pharm. Biomed. Anal. 28 (2002) 209–215.
[22] T.I. Ruo, Z. Wang, M.S. Dordal, A.J. Atkinson Jr., Assay of inulin in biological fluids by high-performance liquid chromatography with pulsed amperometric detection, Clin. Chim. Acta 204 (1991) 217–222.
[23] H.F. Kuehnle, K. von Dahl, F.H. Schmidt, Fully enzymatic inulin determination in small volume samples without deproteinization, Nephron 62 (1992) 104–107.
[24] S. Campuzano, R. Gálvez, M. Pedrero, F.J. Manuel de Villena, J.M. Pingarrón, Preparation, characterization, and application of alkanethiol self-assembled monolayers modified with tetrathiafulvalene and glucose oxidase at a gold disk electrode, J. Electroanal. Chem. 526 (2002) 92.
[25] A.S. Bassi, E. Lee, J.X. Zhu, Carbon paste mediated, amperometric, thin film biosensor for fructose monitoring in honey, Food Res. Intl. 1 (1998) 119–127.
[26] P.A. Paredes, J. Parellada, V.M. Fernández, I. Katakis, E. Domínguez, Amperometric mediated carbon paste biosensor based on D-fructose dehydrogenase for the determination of fructose in food analysis, Biosens. Bioelectron. 12 (1997) 1233–1243.
[27] M. Darder, E. Casero, F. Pariente, E. Lorenzo, Biosensors based on membrane-bound enzymes immobilised in a 5-(octyldithio)-2-nitrobenzoic acid layer on gold electrodes, Anal. Chem. 72 (2000) 3784–3792.

[28] J. Tkác, I. Voštiar, E. Šturdýk, P. Gemeiner, V. Mastihuba, J. Annus, Fructose biosensor based on D-fructose dehydrogenase immobilised on a ferrocene-embedded cellulose acetate membrane, Anal. Chim. Acta 439 (2001) 39–46.

[29] V. Carralero, M.L. Mena, A. Gonzalez-Cortés, P. Yáñez-Sedeño, J.M. Pingarrón, Development of a high analytical performance–tyrosinase biosensor based on a composite graphite–Teflon electrode modified with gold nanoparticles, Biosens. Bioelectron. 22 (2006) 730–736.

[30] X. Luo, A. Morrin, J. Killard, M.R. Smyth, Application of nanoparticles in electrochemical sensors and biosensors, Electroanalysis 18 (2006) 319–326.

[31] S. Liu, D. Leech, H. Ju, Application of colloidal gold in protein immobilization, electron transfer, and biosensing, Anal. Lett. 36 (2003) 1–19.

[32] S. Watanabe, I. Kubo, Fructose biosensor based on D-fructose dehydrogenase and phenanthroline cobalt complex as a mediator, Electrochemistry 70 (2002) 258–263.

[33] L.H. Zhang, C.X. Zhao, D.C. Zhu, Y. Ohta, Y.J. Wang, Purification and characterization of inulinase from *Aspergillus niger* AF10 expressed in *Pichia pastoris*, Protein Express. Purif. 35 (2004) 272–275.

[34] J. Castillo, S. Gáspár, I. Sakharov, E. Csöregi, Bienzyme biosensors for glucose, ethanol, and putrescine built on oxidase and sweet potato peroxidase, Biosens. Bioelectron. 18 (2003) 705–714.